Fibers and Polymers
https://doi.org/10.1007/s12221-023-00022-0

Online ISSN 1875-0052
Print ISSN 1229-9197

REGULAR ARTICLE

Potential of Titanium Dioxide to Remove Bromothymol Blue (BTB) in Aqueous Solution by Batch Mode Adsorption–Kinetic, Isotherm and Thermodynamic Studies

Moussa Abbas[1,2]

Received: 14 November 2020 / Revised: 14 January 2021 / Accepted: 20 January 2021

Abstract
The adsorption is widely used to remove certain classes of pollutants from water, especially those that are hardly biodegradable and dyes represent one of these problematic groups. The removal of bromothymol blue (BTB) from wastewater using TiO_2 was studied in batch system. The adsorbent TiO_2 has a specific surface area of 400 m^2/g, a mean crystallites sizes (5–10 nm), and pH_{pzc} equal to 6.5. TiO_2 is stable over the whole pH range and constitutes a good compromise between efficiency and stability (in both acidic and basic media), therefore, the use of other additives is not necessary. Its non-toxicity and low energy required for its activation ($E \sim 3$ eV) as well as its low cost for most of the applications envisaged make it advantageous. The influence of effective variables such as solution pH (1–10), contact time (0–60 min), initial BTB concentration (5–40 mg/l), adsorbent dose of TiO_2 (0.2–2 g/l), and temperature (20–60 °C) on the adsorption efficiency was examined, while the BTB content was determined by UV–Vis spectrophotometry. The optimal pH, adsorbent dose, and contact time for the efficient removal were found to be 10, 0.2 g/l, and 30 min, respectively, and the adsorbent was characterized by the BET analysis and point of zero charge (pH_{pzc}). Among the different kinetic models, the experimental data of the BTB removal are well fitted with the pseudo-first-order kinetic model with a high determination coefficient. The evaluation of the fitness of equilibrium data by various conventional isotherm models, based on the R^2 value as criterion, show the successful applicability of the Langmuir model for the interpretation of experimental data with a maximum adsorption capacity (q_{max}) of 27.02 mg/g at 20 °C and R^2 of 0.997. The adsorption isotherms at different temperatures have been used for the determination of the free energy ($\Delta G^o = 2.1808$ to—1.0981 kJ/mol), enthalpy ($\Delta H^o = 20.74$ kJ/mol), and entropy ($\Delta S^o = 65.58$ J/mol/K) indicate that the overall adsorption is spontaneous and endothermic in nature.

Keywords Adsorption · Kinetics · Modeling · Diffusion · Thermodynamic · Bromothymol blue (BTB) · Titanium dioxide · Isotherm

1 Introduction

The discoloration of residual dyes in industrial wastewaters has received considerable attention due to aesthetic reasons, decreased photosynthesis activity of the aquatic flora and recalcitrance and hazardous nature of many dyes. In this respect, Bromothymol blue (BTB), a triphenylmethane dye, frequently used for dyeing in the textile industry, is considered to be harmful as it may cause damage to lungs and mucous membranes, if ingested, and skin/eye irritation when in contact. Prolonged exposure may also lead to target organ damage. Water contamination by organic pollutants is a serious issue because of their acute toxicity and carcinogenic nature. They present a serious threat to the living beings [1], mainly because most organic pollutants contain aromatic rings with mesomeric effects, known to enhance the accumulation and in this way the difficulty to remove from water bodies [2]. Usually, agricultural organic pollutants, such as pesticides and fertilizers, contaminate the aquatic medium by watering plants. Likewise, the hydrocarbons, phenols,

✉ Moussa Abbas
moussaiap@gmail.com; m.abbas@univ-boumerdes.dz

[1] Laboratory of Soft Technologies, Valorization, Physicochemistry of Biological Materials and Biodiversity (LTDVPMBB), Faculty of Sciences, University M'hamed Bougara of Boumerdes, 35000 Boumerdes, Algeria

[2] Laboratory of Applied Chemistry and Materials (LabCAM), University of M'hamed Bougara of Boumerdes, 35000 Boumerdes, Algeria

Published online: 03 February 2023

plasticizers, biphenyls, detergents, and dyes were discharged anarchically in the water bodies as industrial effluents. Apparently, the dyes present a particular source of organic water contamination, because they are highly consumed in coloring textiles and fabrics [3].

Typically, they have relatively a high solubility in water as a result of the ionic or hydrophilic nature, where even very low concentrations in water could be highly hazardous to plant and marine organisms [4]. Unfortunately, these dyes are stable to light, heat, biodegradation or aerobic digestion [5]. Moreover, they also added color to the water body that screened the sunlight from passing through, and consequently subsiding the photochemical and biological activities of the aquatic life [6].

Most dyes are applied in aqueous solutions, and may require a mordant to improve their fastness on fibers [7]. Direct skin contact of dyes can also result in various types of health problems like hypersensitivity, mutagenic and carcinogenic effects, allergy and asthma, skin eczema, and immune suppressive effects. This leads us to worry about their use as well as their removal from aqueous solutions [8]. Currently, numerous water treatments [9], such as electrocoagulation [10], membrane separation, advanced oxidation processes (AOPs) [11], photocatalytic degradation [12–25] and adsorption [26–34] are in use. However, most of them have inherent drawbacks like economic viability, incomplete partial removal of recalcitrant and non-biodegradable dyes, and formation of undesirable by products. On the contrary, the adsorption remains an attractive process for the water treatment due to its ease of use, simplicity of design, and cost effectiveness. The objectives of this study are as follows:

- To contribute to the reduction of environmental pollution, which remains a major international problem
- To carry out tests on an industrial scale.
- Application of non-toxic TiO_2 as semiconductor without treatment in the field of water treatment. TiO_2 can be regenerated for other various applications.
- The elimination of pollutants by the heterogeneous solar photodegradation in the presence of TiO_2 is the next step in this work.

2 Experimental

2.1 Materials

2.1.1 Adsorbate BTB

Bromothymol blue (BTB), also called 3′,3″-dibromothymolsulfonphthalein (chemical formula $C_{27}H_{28}Br_2O_5S$) is a pH-sensitive synthetic dye (Fig. 1) used as indicator

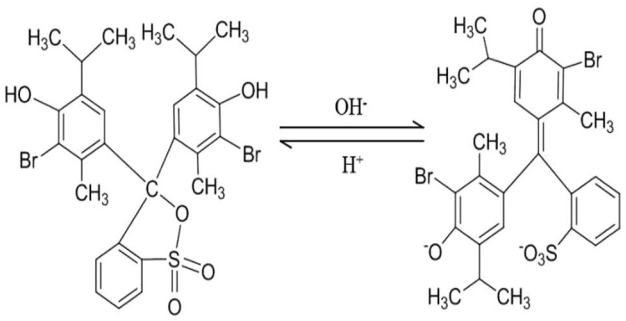

Fig. 1 Structure of bromothymol blue (BTB)

Table 1 Properties of the dye BTB

Brute formula	$C_{27}H_{28}Br_2O_5S$
Molecular weight (g/mol)	624.38
Composition (%)	C: 51.74, Br: 25.59, H: 4.52, O: 12.52, S: 5.14
Name:	Bromothymol blue (BTB)
Wavenumber λ_{max} (nm)	432
Solubility in water (g/*l*)	10 at $T = 25$ °C
Relative volumic mass	1.25
Melting temperature (°C)	204
pKa	7.1

[35–37]. It is negatively charged in alkaline solution and its physical and chemical properties are summarized in Table 1. BTB is a colorful pH indicator, with a pale yellow below pH 6, and blue above pH > 7.6 and can be used as a blue dye in a neutral environment; its turning zone is in the range (6 < pH < 7.6) with a green color. BTB is also used as a colored marker to verify the progress of the electrophoresis on polyacrylamide gel or an electrophoresis. A quantity of BTB powder was accurately weighed and diluted with ultra-pure water in a volumetric flask of volume relative to the concentration which one wishes to prepare 100 mg/l; this preparation was followed by homogenization on a magnetic stir plate. The initial pH of BBT solutions was modified in order to study the effect of this parameter on the discoloration rate by adding few drops of H_2SO_4 or NaOH. The pH was accurately measured with a digital HANNA pH meter (Model HI 8521).

At pH 6.3, the absorption spectrum of BTB (Fig. 2) shows a single band in the visible region ($\lambda_{max} = 432$ nm), and two bands in the UV region (272 and 332 nm). An acidic pH (= 3) does not affect significantly the absorption spectrum of BTB. Conversely, in a basic medium (pH = 10), a bathochromic shift was observed from the main band at 612 nm with a significant increase in the molar absorption and two bands in the UV region are shifted toward 300 and 388 nm.

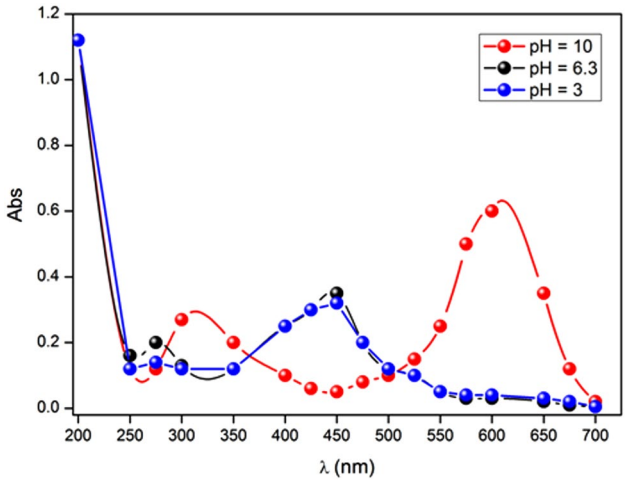

Fig. 2 UV–Visible absorption spectra of BTB (10 mg/l) in aqueous solution at different pHs

Table 2 Physicochemical properties of TiO_2

Composition	80% Anatase	20% Rutile
Eg (eV)	3.1	3.2
ρ (g/cm^3)	4.25	3.85
ΔG_f (kcal/mol)	− 212.8	− 211.5
pH_{zpc}	6.3	
Surface area (m^2/g)	400	
Crystal size (nm)	21	

2.1.2 Adsorbent TiO2

TiO_2 was purchased from Ahlstrom firm and consists of PC25 Titania by Millennium Inorganic Chemicals with a specific surface area 55 m^2/g and an average crystallites size of 20 nm. The physicochemical characteristics are given in Table 2. The pH determines the surface properties of solids and the state of the pollutant as a function of its pKa and characterizes the water to be treated. Generally, when a compound is partially ionized or carrying charged functions, it is imperative to consider the electrostatic interactions that occur with TiO_2. Indeed, according to the zero charge point (pH_{pzc}), the surface charge of the oxide depends on pH. Thus, for TiO_2, the surface is positively charged below pH_{pzc} (=6.5) related to the fixation of protons, and negatively charged above pH_{pzc} [38]. Therefore, the surface charge influences the dye adsorption and can promote or limit the adsorption.

2.2 UV–Visible Spectrophotometry

The spectrophotometry is a useful method which owes its development to progress in the quantum mechanics. It allows us to identify a chemical substance and to determine the concentration of a solute in a solution by the interaction of the electrons of the molecules of the solute (chromophore) with incident light. The Lambert–Beer law gives the absorbance (A):

$$A = \varepsilon_{\lambda} \cdot C \cdot L, \tag{1}$$

where L is the optical path (cm), C is the molar concentration of BTB and ε_{λ} is the extinction coefficient of the chromophore, which is wavelength (λ) dependent. 10 mm quartz cell was used and the results were reproducible at 0.1 nm, while the scanning rate was set at 1200 nm/min. Two light sources were used: a visible tungsten halogen lamp and a UV deuterium lamp. The blanks were carried out in a quartz cell identical to the previous one with ultrapure water. Measurements of residual concentrations were obtained by linear interpolation from a previously calibrated graph.

2.3 pH Measurement

The pH was reliably measured using a microprocessor-based pH meter of the HANNA HI 8521 type. The instrument was calibrated with commercial buffers of pH 4, pH 7, and pH 10. The pH was adjusted to different values for acidic media using H_2SO_4 and NaOH for basic solutions.

2.4 Adsorption Experiments

The BTB adsorption studies on TiO_2 were realized in a 50 ml reactor homogeneously stirred by a magnetic stirrer. The temperature was controlled by water circulation in the jacket of the reactor by using a thermostated bath. The BTB solution (50 ml) at a desired concentration was introduced into the reactor with a given mass of TiO_2 as catalyst. The adsorption kinetics began at the initial instant ($t=0$ min) where the sample was immediately withdrawn. Then, the suspensions were taken with a syringe at regular contact times and immediately filtered through 0.45 µm Millipore filters; the BTB concentrations were analyzed by UV–Visible spectrometry in a the λ-range (200–800 nm). The adsorption capacity of TiO_2 is defined as the quantity of substrate (mass or volume) adsorbed per unit weight of adsorbent at a given temperature. It takes into account many parameters for the adsorbate (size of the molecules, solubility in water, etc.) as well as for the adsorbent (specific surface, structure and type of particles, the constituent, etc.).

The effects of the experimental parameters namely the initial BTB concentration C_0 (5–40 mg/l), pH (2–12), adsorbent dosage (0.2–2 g/l), agitation speed (100–300 rpm), and temperature (20–60 °C) on the BTB removal is studied in batch mode for a specific contact time (0–60 min). The

stock solution was daily prepared by dissolving the accurate amount BTB (99%) in distilled water, the working solutions were made up by dilution. The amount q_t (mg/g) and yield R (%) of adsorbed BTB onto TiO_2 (q_t) were calculated from the relations:

$$q_t = \frac{(C_0 - C_t) \bullet V}{m} \tag{2}$$

$$R(\%) = \frac{(C_0 - C_t)}{C_0} \times 100, \tag{3}$$

where C_0 is the initial BTB concentration and C_t is the concentrations (mg/l) at time t, V is the volume of solution (l), and m is the mass of TiO_2 (g).

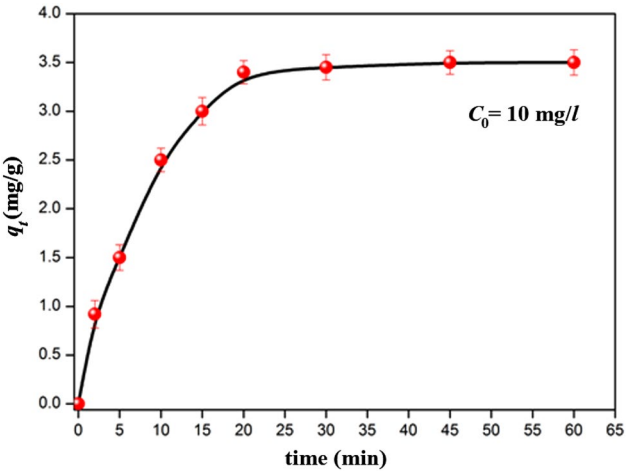

Fig. 3 Evolution of the adsorbed quantity of BBT over the time on TiO_2-P25: ([BTB] = 10 mg/l, pH = 6.3, [TiO_2] = 1 g/l, and T = 20 °C)

3 Results and Discussion

Bromothymol blue has been widely used in fuel cells, paints, cleaning products, detergents, and textiles. It is considered dangerous and causes serious eye damage that can impair fertility, with genetic abnormalities, in case of prolonged exposure. It also causes damage to the ecosystem due to its high stability [39]. As a result, an environmentally benign removal of bromothymol blue from industrial effluents is of crucial importance. The natural, non-toxic, hydrophilic, biocompatible, and biodegradable sphagnum peat moss solid provided a useful substance for the environmentally friendly adsorption removal of bromothymol from water. Here in the dye removal was thoroughly inspected at different conditions of pH, contact time, adsorbate initial concentration and adsorbent dose.

3.1 Determination of the Adsorption Equilibrium Time

The knowledge of the time after which the adsorption/desorption equilibrium is reached is necessary to determine the various points constituting the isotherm as well as its nature. Since the adsorption transfers the pollutant from the liquid to the solid phase, the time between the two phases acts as a limiting factor. The study consists of bringing into contact, in a reactor (200 ml capacity), a volume of 50 ml of BTB solution (10 mg/l) and 1 g/l of the catalyst (TiO_2); the suspension is stirred at 300 rpm at 20 °C. The results of the change in the adsorbed amount of BTB on the catalyst against the contact time are shown in Fig. 3. It can be seen that the equilibrium is reached after only 30 min. The adsorption rate is rapid at the start of the process after 15 min and slows down over the course of the stirring time, reaching equilibrium at 30 min. This is related to the availability of free active support sites at the beginning of the experiment, which becomes weak as time passes. The adsorption capacity of the substrate on TiO_2 is dependent on the surface and structural properties of the catalyst such as the crystallographic composition, the surface area, the particle size distribution, and the porosity.

3.2 Factors Influencing the Adsorption Efficiency of the Dye on the Catalyst

The adsorption of an organic compound on a solid depends on physicochemical parameters, in particular the temperature, the pH, and the dye concentration. The thermodynamic equilibrium between the free species and those adsorbed by the solid is achieved with a more or less slow rate, depending on the nature of both the adsorbent and adsorbate. Other factors (solubility, structure, molecular mass, pKa, charge, polarity) and the experimental conditions of the analytical system also influence the dye adsorption to a less extent.

3.2.1 Influence of Catalyst Concentration

In order to evaluate the optimum TiO_2 content for the BTB adsorption, experiments were carried out in solutions of 10 mg/l, to which catalysts amounts were added in the interval (0.2–2 g/l).The change in the adsorbed BTB amount over the contact time, as a function of the TiO_2 dose, is shown in Fig. 4. It is found that the adsorbed amount decreases with the addition of TiO_2 of 1.2 g/l, beyond which the amount no longer changes. This may be due to the number of adsorption sites which increases with raising the quantity of adsorbent up to 1.2 g/l at which the number of sites becomes stable [40, 41] such behavior can be explained by the following points:

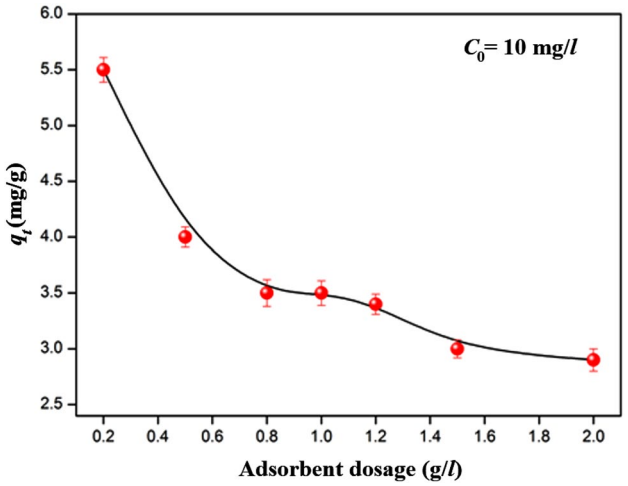

Fig. 4 Influence of the concentration of the TiO_2-P25 catalyst on the adsorption of BTB: ([BTB] = 10 mg/l, pH = 6.3, and T = 20 °C)

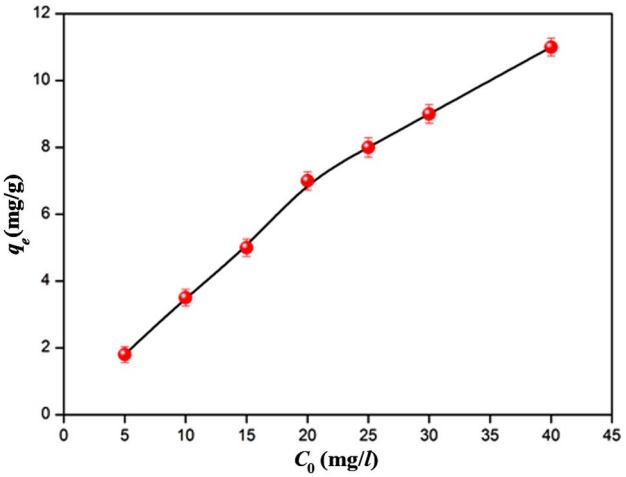

Fig. 5 Influence of the initial BTB concentration on the adsorption by the catalyst TiO_2-P25: ([TiO_2] = 1 g/l, pH = 6.3, and T = 20 °C)

i. As long as the TiO_2 amount added to the solution is small, the BTB molecules can easily access to adsorption sites. The addition of adsorbent increases the number of adsorption sites but the charges of the dye (according to its functional groups) have more difficulty approaching these sites because of the bulk (the electrical state of the surface semiconductor with dye);
ii. A large amount of TiO_2 creates agglomerations of particles, resulting in a reduction in the total adsorption area and, therefore, a decrease in the amount of adsorbate per unit mass of adsorbent.

3.2.2 Influence of the Initial Dye Concentration

Figure 5 shows the influence of the initial BTB concentration C_0 on the adsorption capacity on the TiO_2 surface. We notice a rapid adsorption, where the saturation is reached after only 30 min with the formation of a monolayer. Note that the adsorption capacity increases with augmenting the BTB concentration; this is due to the fact that the diffusion of BTB molecules from the solution toward the adsorbent surface is accelerated at high BTB concentration C_0 [42]. With raising the initial concentration C_0 (5–40 mg/l), the adsorption increases from 2 to 11 mg/g, and we can deduce that the adsorption of BTB onto TiO_2 occurs in three stages:

a) Fast BTB adsorption due to the presence of free sites on the adsorbent surface, which translates the linear increase of the adsorption capacity over time.
b) Reduction of the adsorption rate, evidenced by a small increase in the adsorption capacity attributed to the decrease in the quantity of BTB in solution and the number of available unoccupied sites.
c) Stability of the adsorption capacity is observed, presumably due to the total occupation of adsorption sites: the establishment of the level, therefore, reflects this stage. The adsorption capacity of BTB increases over time reaches a maximum after 30 min and thereafter tends toward a constant value indicating that no more BTB ions are removed from the solution.

3.2.3 Influence of pH

The adsorption is a surface phenomenon and, therefore, depends strongly on the characteristics of the adsorbent surface, which are related to both the morphology and the charge. The net surface charge is conditioned by the nature of the functional groups present therein, which are a combination of positively and negatively charged groups. In fact, at low pH, the predominance of H_3O^+ in solution favors the neutralization of negative surface charges and the net surface charge becomes positive. Conversely, the net surface charge at high OH^- is negative. Monitoring the evolution of the surface load shows that it goes through a state of neutrality, known as the zero point charge (pH_{pzc}). Indeed, pH_{pzc} represents the border where the surface charge is zero and changes sign.

pH_{pzc} of TiO_2 is equal to pH 6.5 [43]. The pH is linked to the ionization state of the catalyst surface according to the following reactions [44]:

$$\mathbf{TiOH + H^+ \longrightarrow TiOH_2^+} \quad \mathrm{pH} < 6.5$$

$$\mathbf{TiOH + HO^- \longrightarrow TiO^- + H_2O} \quad \mathrm{pH} > 6.5$$

The charge of TiO_2 surface is positive in acidic solution, due to the fixation of protons and negatively in basic

medium. Therefore, the surface charge influences the BTB adsorption and can limit the adsorption.

The influence of the pH on the BTB adsorption was studied in the pH range (1–12), by adjusting the solutions to the desired values, by H_2SO_4 or NaOH, while maintaining constant the initial BTB concentration C_0 at 10 mg/l in the presence TiO_2 (1 g/l), a temperature of 20 °C, and a stirring speed of 300 rpm. Figure 6 reports the change of the adsorbed quantity (q_{ads}) of BTB on TiO_2 as a function of the pH. The adsorbed BTB quantity is proportional to the pH in the region (2–10) and a total discoloration is observed at pH 12. The optimal adsorption capacity is obtained at pH 10. BTB shows that the adsorption capacity on TiO_2 increases with raising pH until reaching a maximum in the pH region (8–10), beyond which a sharp decrease is observed in the adsorbed amount. This behavior should give relatively high pKa value (=7.1) of BTB compared to other studied dyes. In alkaline medium, there is similarly a repulsion between the negatively charged molecules of BTB and TiO_2. Therefore, the adsorption maxima was obtained for a pH lying between 8 and 10 range (8–10), the exact value of which differs from one catalyst to another depending on the nature of the interactions with the adsorbent molecules.

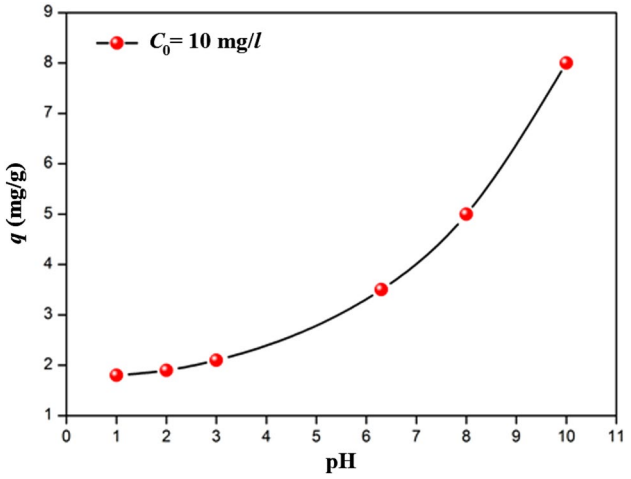

Fig. 6 Evolution of the adsorbed BTB amount on TiO_2-P25 as a function of pH: ([BTB] = 10 mg/*l*, [TiO_2] = 1 g/l, and T = 20 °C)

3.3 Adsorption Kinetic Study

Several models were proposed to study the mechanisms controlling the adsorption. In this study, the experimental data of BTB adsorption are examined using the pseudo-first and pseudo-second-order kinetic model given respect, respectively, by [45, 46]:

$$\log\left(q_e - q_t\right) = \log q_e - \frac{K_1}{2.303} \bullet t \tag{4}$$

$$\frac{t}{q_t} = \frac{1}{K_2 \bullet q_e^2} + \frac{1}{q_e} \bullet t, \tag{5}$$

where q_t is (mg/g) is the amount of adsorbed BTB on TiO_2 at the time t (min); $K_1(\text{min}^{-1})$ and K_2 (g/mg/min) are the pseudo-first order and pseudo-second-order kinetics constants, respectively. The slope and intercept of the lines $\log\left(q_e - q_t\right)$ vs. t and t/q_t vs. t were used to compute the constants K_1, K_2, and q_e. The rate constant of the dye adsorption, the predicted dye uptakes, the corresponding determination coefficients R^2, and relative error Δq (%) for TiO_2 are summarized in Table 3. However, for the pseudo-second-order kinetic (Fig. 7), the experimental data deviate from linearity, as evidenced from the small values of q_e and C_0, and therefore, the model is inapplicable for the present system. Conversely, the determination coefficient and $q_{e,cal}$ determined from the pseudo-first order kinetic model agree perfectly with the experimental data (Fig. 7) and its applicability suggests that the adsorption of BTB onto TiO_2 is based on a chemical reaction (chemisorption), involving an exchange of electrons between adsorbent and adsorbate.

The Elovich kinetic equation is related to the chemisorption and is often applied for systems where the

Table 3 Constants of the kinetic models

Pseudo-second order					Pseudo-first order				
C_0(mg/*l*)	q_{exp} (mg/g)	q_{cal}(mg/g)	R^2	Δq (%)	K_2 (g/mg/min)	q_{cal} (mg/g)	R^2	Δq (%)	K_1 (min^{-1})
10	3.5	3.93	0.998	10.09	0.046	3.76	0.96	6.90	1.326
Elovich					Intra-particle diffusion				
C_0(mg/l)	R^2	β (mg/g)	α (mg/g/min)		C_0 (mg/l)	K_{id}(mg/g/$\text{min}^{1/2}$)	R^2	C (mg/g)	
10	0.905	1.185	1.425		10	1.262	0.9991	0.146	

Δq (%) = $[(q_{cal—}q_{exp})/q_{cal}] \times 100$

q_{cal} (mg/g): Calculated adsorbed quantity

q_{exp} (mg/g): Experimental adsorbed quantity

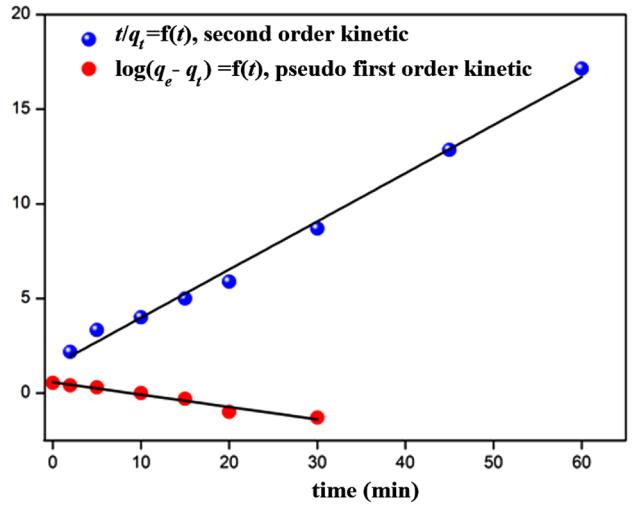

Fig. 7 Modeling of the pseudo-first and second-order kinetics

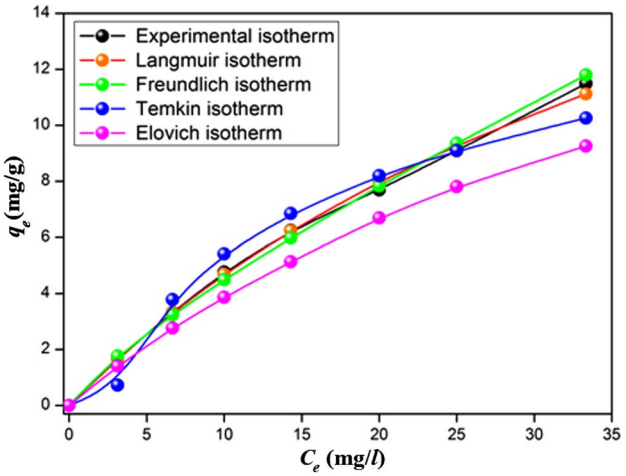

Fig. 8 Adsorption isotherms under optimal conditions for the different applied models: ([BTB] = 5–40 mg/l, pH = 6.3, [TiO_2] = 1 g/l, and T = 20 °C)

adsorbent surface is heterogeneous [47]; the linear form is expressed by:

$$q_t = \left(\frac{1}{\beta}\right)\ln(\alpha \bullet \beta) + \left(\frac{1}{\beta}\right)\ln t, \tag{6}$$

where α (mg/g/min) is the initial adsorption rate constant and β (mg/g) is the constant associated with the relationship between the degree of surface coverage and the activation energy involved in the chemisorption.

3.4 Intra-particle Diffusion Equation

The intra-particle diffusion model [48] during the transportation of adsorbate from solution to the surface was also investigated:

$$q_t = K_{id}\sqrt{t} + C, \tag{7}$$

where K_{id} is the intra-particle diffusion rate constant (mg/g/min$^{1/2}$), q_t is the amount of BTB adsorbed at time t, and C (mg/g) is the intercept. The plot of q_t against $\sqrt{t}$ enables us to calculate both K_{id} and C. It presents a multi-linearity correlation, which indicates that two steps occur during the BTB adsorption.

- The mechanism of adsorption is complex, but the intra-particle diffusion is important in the early stages.
- The first linear portions could be due to intra-particle diffusion effects.
- The slopes of the linear parts are defined as rate parameters, characteristic of the adsorption rate in the region where the intra-particle diffusion is successfully applied.

After saturation of the surface, the BTB molecules enter inside the adsorbent by intra-particle diffusion in the pores and internal surface diffusion until the equilibrium is reached, represented by the second lines. The constants of the different models deduced after modeling, determination coefficient R^2 and relative error Δq (%) = $[(q_{cal\_}q_{exp})/q_{cal}] \times 100$ are gathered in Table 3.

3.5 Adsorption Equilibrium Isotherms

To assess the TiO_2 performance, different isotherms, which were defined by Langmuir [49], Temkin [50], Freundlich [51], and Elovich [52], were tested in the present case (Fig. 8). Besides, the models were applied at optimal conditions of the parameters.

The Langmuir model remains the most popular and widely applied. It is represented by the non-linear (Eq. (8a)) and linear (Eq. (8b)) forms:

$$q_e = \frac{q_{\max} \bullet K_L \bullet C_e}{1 + K_L \bullet C_e} \tag{8a}$$

$$\frac{1}{q_e} = \frac{1}{q_{\max}} + \frac{1}{q_{\max} \bullet K_L \bullet C_e}, \tag{8b}$$

where q_e is the amount of absorbate adsorbed per gram of the adsorbent at equilibrium (mg/g),C_e is the equilibrium concentration of absorbate (mg/l), $q_{\max}$ the maximum monolayer adsorption capacity (mg/g), and $K_L$is the Langmuir isotherm constant (l/mg) related to the free adsorption energy. The values of $q_{\max}$ and K_L are obtained from the slope and intercept of the plot of $1/q_e$ vs. $1/C_e$, respectively.

The Temkin isotherm describes the adsorption on heterogeneous surfaces, and is expressed in the following form:

$$q_e = \left(RT/b_T\right) \bullet \ln\left(A_T C_e\right) = \left(RT/b_T\right)\ln A_T + \left(RT/b_T\right)\ln C_e, \quad (9)$$

where A_T is Temkin isotherm equilibrium binding constant (l/mg), b_T is the Temkin isotherm constant, R universal gas constant (8.314 J/mol/K), and T temperature (293 K). The data are analyzed according to Eq. (9) and the plot of q_e vs.lnC_e allows to determine the constants A_T and b_T.

The Freundlich isotherm is valid for non-ideal adsorption on heterogeneous surfaces as well as multilayer sorption.

$$q_e = K_F C_e^{1/n}. \quad (10)$$

The Freundlich constant K_F characterizes the adsorption capacity of the adsorbent (l/g) while n is an empirical constant related to the magnitude of the adsorption driving force. Therefore, the plot lnq_e vs.lnC_e enables the determination of both the constant K_F and n.

The Elovich isotherm assumes that the number of adsorption sites augments exponentially with the adsorption and this implies a multilayer adsorption described by:

$$\frac{q_e}{q_{\max}} = K_E C_e \exp\left(-\frac{q_e}{q_{\max}}\right) \quad (11a)$$

$$\ln\frac{q_e}{C_e} = \ln\left(K_E q_{\max}\right) - \frac{q_e}{q_{\max}}, \quad (11b)$$

where K_E(l/mg) is the Elovich constant at equilibrium, $q_{\max}$ (mg/g) the maximum adsorption capacity, q_e(mg/g) the adsorption capacity at equilibrium, and C_e (g/l) the concentration of the adsorbate at equilibrium. Both the equilibrium constant and maximum capacity are computed from the plot of $\ln\frac{q_e}{C_e}$ vs. q_e. The constants of all models deduced after modelling are listed in Table 4.

3.6 Influence of Temperature

The temperature is an important parameter that influences the adsorption of solutes such as the dyes to the surface of oxides. Its importance is not limited only to the need to understand how it affects adsorption and desorption, but also to the use of experimental results, allowing access to useful thermodynamic information, namely the enthalpy and entropy. They can be evaluated from the modeling of the experimental results with adequate theoretical models. The variation of the adsorbed BTB amount at equilibrium (q_e) as a function of temperature is illustrated in Fig. 9. Note that q_e increases when the temperature increases, indicating that the adsorption has an endothermic nature (chemisorption).

3.7 Thermodynamic Characterization of Adsorption

The adsorption capacity of BTB augments with raising temperature over the range (20–60 °C), above which the vaporization becomes an increasing handicap. The insights of the adsorption mechanism are highlighted from the thermodynamic study through the calculation of the free energy ($\Delta G°$), enthalpy ($\Delta H°$), and entropy ($\Delta S°$).

The thermodynamic equilibrium constant (K_d) is determined by plotting $\ln\frac{q_e}{C_e}$ vs.q_e and extrapolating to zero q_e[53]:

$$\Delta G° = \Delta H° - T\Delta S° \quad (13)$$

$$\Delta G° = -RT \bullet \ln K_d \quad (14)$$

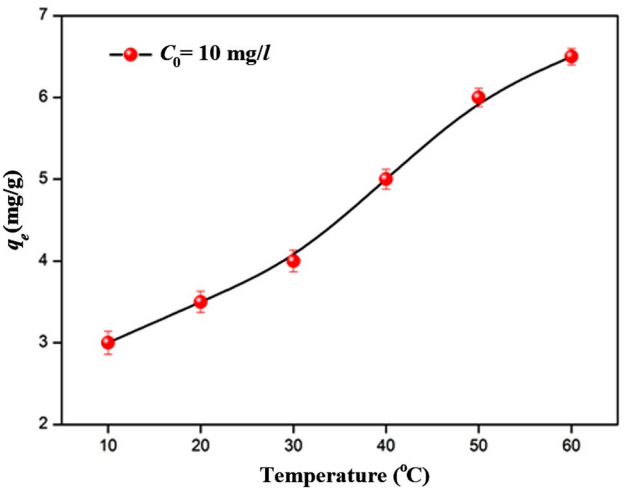

Fig. 9 Influence of temperature on adsorption capacity: ([BTB] = 10 mg/l, [TiO_2] = 1 g/l, and pH = 6.3)

Table 4 Constants of the isotherms models

20 °C	Langmuir	Freundlich	Temkin	Elovich
	K_L: 0.021 l/mg $q_{\max}$: 27.02 mg/g	1/n: 0.803 n: 1.24 K_F: 0.706 mg/g	b_T: 4.029 A_T: 0.383 l/mg ΔQ: 16.616 kJ/mol	K_E: 0.024 l/mg $q_{\max}$: 24.408 mg/g
	R^2: 0.997	R^2: 0.995	R^2: 0.938	R^2: 0.987

R^2 Determination coefficient, ΔQ Temkin Energy

$$\ln K_d = \frac{\Delta H^\circ}{R} \bullet \frac{1}{T} - \frac{\Delta S^\circ}{R}. \quad (15)$$

The plot of $\ln K_d$ vs.$1/T$ (Fig. 10) is linear; the values of ΔH° and ΔS° are obtained from the slope and intercept of the Van't Hoff equation Eq. (15), while the free enthalpy (ΔG°) at various temperatures are reported in Table 5. The negative ΔG° value indicates a non-spontaneous adsorption, while the negative values of ΔH° and ΔS° show that the BTB adsorption on TiO_2 is endothermic with an increased randomness at the solid-solution interface.

3.8 Performance of the TiO_2

It is instructive for a comparative purpose to report the adsorption capacity of some adsorbents available in the literature. The different values of the maximum adsorption capacity (q_{max}) of various adsorbents cited in previous works (Table 6). We can see that the BTB adsorption observed in our study is well positioned compared to other researches with a maximum capacity q_{max} of 27.07 mg/g, relatively interesting. The differences of the dye uptakes are due to the properties of each adsorbent like the structure, functional groups, and surface area. TiO_2 could be an attractive adsorbent for dyes owing to the isoelectric point (pH_{pzc}).The desorption is an unavoidable process and is an intermediate stage toward the adsorbent regeneration. The latter is an essential tool to evaluate the reutilization of any adsorbent for large scales applications, owing to the ecological concerns and needs for sustainable development. This study has given encouraging results. We wish to carry out column adsorption tests under the conditions applicable to the treatment of industrial effluents and to test the photodegradation of BTB on the semiconductor is our main objective in the future. The undertaken preliminary tests were satisfactory; the detailed tests are currently under way and will be consecutively published very soon in a next paper.

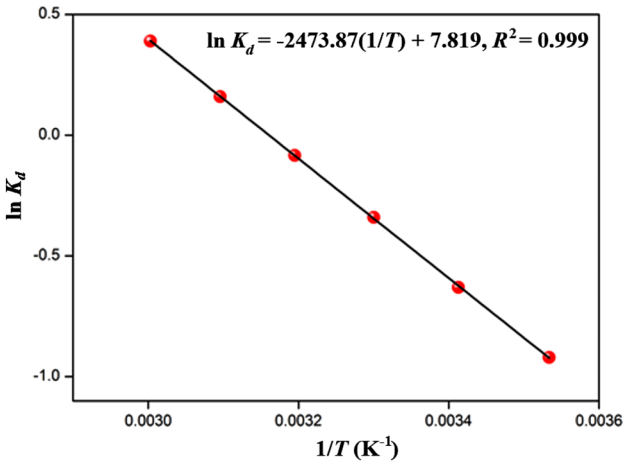

Fig. 10 Linear form of ln K_d as a function of $1/T$ for BTB in the presence of TiO_2-P25: ([BTB] = 10 mg/l, [TiO_2] = 1 g/l, and pH = 6.3)

Table 5 Determination of thermodynamic parameters

T (K)	$1/T$ (K^{-1})	ln K_d	ΔH° (kJ/mol)	ΔS° (J/K/mol)	ΔG° (kJ/mol)
283	0.00353	− 0.92	20.74	65.58	2.1809
293	0.00341	− 0.63			1.5251
303	0.0033	− 0.34			0.8693
313	0.0032	− 0.08			0.2135
323	0.0031	0.16			-0.4423
333	0.003	0.39			-1.0981

4 Conclusion

This contribution has shown that TiO_2 can be successfully employed as efficient adsorbent for the elimination of the bromothymol blue from aqueous solution. The Langmuir models provided the best fit of the equilibrium adsorption data with a maximum adsorption capacity of 27.02 mg/g at 20 °C.

The pseudo-second-order model gave the best description of the kinetic data. The negative free enthalpy (ΔG°) and positive enthalpy (ΔH°) indicated that the BTB adsorption onto TiO_2 is spontaneous and endothermic over the studied temperature range. The positive entropy (ΔS°) states clearly that the randomness increases at the solid-solution interface during the BTB adsorption, indicating that some structural exchange may occur among the active sites of the TiO_2 adsorbent and BTB ions.

The BTB adsorption by TiO_2 follows a pseudo-first-order kinetic model, which relies on the assumption that the chemisorption is the rate-limiting step. The BTB molecules are chemically linked to the adsorbent surface and tend to

Table 6 Comparative study of the maximum adsorption capacity of BTB with literature

Adsorbent	q_{max} (mg/g)	References
TiO_2 adsorbent	27.02	This Study
Carbon nanotubes	55	[54]
Polyvinyl alcohol	276.2	[55]
Chitosan-bamboo sawdust composites	217.39	[56]
Au-NP loaded on activated carbon	95.24	[57]
Raw Maiz Cob	R (%) = 94.39	[58]
Sawdust treated by polyaniline	R (%) = 99	[59]
Latvian Sphagnum Peat Moss	R (%) = 88.2	[60]

find sites that maximize their coordination number with the surface.

The capacity q_{max} is in agreement with those of previous works, suggesting that BTB is easily adsorbed on TiO_2. The present research showed that TiO_2 is potentially an attractive adsorbent for the basic dyes. The study in tiny batch gave rise to encouraging results, and we hope to achieve the adsorption tests in column mode under the conditions applicable to the treatment of industrial effluents.

Acknowledgements The financial support of the work was provided by Boumerdes University, Science faculty, Chemical department.

Declarations

Conflict of Interest The authors attest that there are no conflict of interest and financial, personal, or other relationships with other people, laboratories, or organizations worldwide.

References

1. I. Anastopoulos, G.Z. Kyzas, J. Mol. Liq. **200**, 381 (2014)
2. I. Ali, M. Asim, T.A. Khan, J. Environ. Manag. **113**, 170 (2012)
3. M.T. Yagub, T.K. Sen, S. Afroze, H.M. Ang, J. Colloid, Interface Sci. **209**, 172 (2014)
4. I. Kabdasli, O. Tunay, D. Orhon, Water Sci. Technol. **40**, 261 (1996)
5. M. Mahramanlioglu, M. Zahoor, A. Cinarli, I. Kizilcikli, Fresenius Environ. Bull. **19**, 911 (2010)
6. Y.C. Wong, Y.S. Szeto, W.H. Cheung, G. McKay, Process Biochem. **39**, 695 (2004)
7. B. Saritha, K. Rajasekhar, K. Kiso, *Int. J. Innov. Res. Sci, Eng. Technol.*, **4**, 6821 (2015).
8. K.H. Hassan, E.M. Mahdi, Asian J. Appl. Sci. **4**, 730 (2016)
9. V.K. Gupta, I. Ali, T.A. Saleh, A. Nayak, S. Agarwal, RSC Adv. **2**, 6380 (2012)
10. I. Ali, T.A. Khan, M. Asim, Sep. Purif. Rev. **40**, 25 (2011)
11. S. Karthikeyan, V.K. Gupta, R. Boopathy, A. Titus, G. Sekaran, J. Mol. Liq. **173**, 153 (2012)
12. T.A. Saleh, V.K. Gupta, J. Colloid Interface Sci. **371**, 101 (2012)
13. M. Abbas, M. Trari, Desalin. Water Treat. **180**, 398 (2020)
14. M. Abbas, M. Trari, Scientific African **8**, e00387 (2020)
15. Y.-H. Chiu, T.-F. Mark Chang, C.-Y. Chen, M. Sone, and Y.-J. Hsu, *Catalysts*, **9**, 430 (2019).
16. M.-J. Fang, C.-W. Tsao, Y.-J. Hsu, J. Phys. D: Appl. Phys. **53**, 143001 (2020)
17. Y.-H. Chiu, Y.-J. Hsu, Nano Energy **31**, 286 (2017)
18. Y.C. Pu, H.-Y. Chou, W.-S. Kuo, K.-H. Wei, Y.-J. Hsu, Appl. Catal. B: Environ. **204**, 21 (2017)
19. Y.C. Pu, W.-H. Lin, Y.-J. Hsu, Appl. Catal. B: Environ. **163**, 343 (2015)
20. Y.-D. Chiou, Y.-J. Hsu, Appl. Catal. B: Environ. **105**, 211 (2011)
21. Y.-F. Lin, Y.-J. Hsu, Appl. Catal. B: Environ. **130–131**, 93 (2013)
22. M.-Y. Chen, Y.-J. Hsu, Nanoscale **5**, 363 (2013)
23. R. Saravanan, E. Sacari, F. Gracia, M.M. Khan, E. Mosquera, V.K. Gupta, J. Mol. Liq. **221**, 1029 (2016)
24. M. Ghaedi, S. Hajjati, Z. Mahmudi, I. Tyagi, S. Agarwal, A. Maity, V.K. Gupta, Chem. Eng. J. **268**, 28 (2015)
25. S. Rajendran, M.M. Khan, F. Gracia, J. Qin, V.K. Gupta, S. Arumainathan, Sci. Rep. **6**, 31641 (2016)
26. M. Abbas, Adsorpt. Sci. Technol. **38**, 24 (2020)
27. M. Abbas, Z. Harrache, M. Trari, J. Eng. Fiber. Fabr. **15**, 1 (2020)
28. M. Abbas, Mater. Today: Proc. **31**, 437 (2020)
29. M. Abbas, J. Water Reuse Desalin **10**, 251 (2020)
30. M. Abbas, M. Trari, Fibers Polym. **21**, 810 (2020)
31. M. Abbas, Z. Harrache, M. Trari, Adsorpt. Sci. Technol. **37**, 566 (2019)
32. E.A. Dil, M. Ghaedi, A.M. Ghaedi, A. Asfaram, A. Gourdarzi, S. Hajati, M. Soylak, S. Agarwal, V.K. Gupta, J. Ind. Eng. Chem. **34**, 186 (2016)
33. Suhas, V. K. Gupta, P. J. M. Carrott, R. Singh, M. Chaudhary, and S. Kushwaha, *Bioresour. Technol.*, **216**, 1066 (2016).
34. A.E. Burakov, E.V. Galunin, I.V. Burakova, A.E. Kucherova, S. Agarwal, A.G. Tkachev, V.K. Gupta, Ecotoxicol. Environ. Saf. **148**, 702 (2018)
35. X. Liu, S.Q. Zhang, X. Wei, T. Yang, M.L. Chen, J.H. Wang, Biosens. Bioelectron. **109**, 150 (2018)
36. C. Rukchon, A. Nopwinyuwong, S. Trevanich, T. Jinkarn, P. Suppakul, Talanta **130**, 547 (2014)
37. L. Gao, X. Yang, Y. Shu, X. Chen, J. Wang, J. Colloid Interface Sci. **512**, 819 (2018)
38. M. Abbas, T. Aksil, M. Trari, Desalin. Water Treat. **125**, 93 (2018)
39. S. Agarwal, H. Sadegh, M. Monajjemi, A.S. Hamdy, G.A.M. Ali, A.O.H. Memar, S. Ghoshekandi, R. Tyagi, V.K. Gupta, J. Mol. Liq. **218**, 191 (2016)
40. V.K. Gupta, A. Mittal, V. Gajbe, J. Colloid Interface Sci. **284**, 89 (2005)
41. W.-T. Tsai, H.-C. Hsu, T.-Y. Su, K.-Y. Lin, C.-M. Lin, T.-H. Dai, J. Hazard. Mater. **147**, 1056 (2007)
42. Z. Harrache, M. Abbas, T. Aksil, M. Trari, Desalin. Water Treat. **147**, 273 (2019)
43. T. Sauer, G. Cesconeto Neto, H. J. José, and R. F. Moreira, *J. Photochem. Photobiol. A: Chem.*, **149**, 147 (2002).
44. M.H. Habibi, A. Hassanzadeh, S. Mahdavi, J. Photochem. Photobiol. A: Chem. **172**, 89 (2005)
45. Y. S. Ho and G. McKay, *Trans IChemE,* **76**, Part B, 183 (1998).
46. R.S. Juang, M.L. Chen, Ind. Eng. Chem. Res. **36**, 813 (1997)
47. G. Woodbury, *Physical Chemistry* (Brooks/Cole Publishing Company, New York, 1997), p.820
48. W. J. Weber and J. C. Morris, *J. Sanit. Eng. Div., Am. Soc. Civ. Eng.*, **89**, 31 (1963).
49. I. Langmuir, J. Am. Chem. Soc. **40**, 1361 (1918)
50. M. Temkin, V. Pyzhev, Acta Physicochim. URSS **12**, 327 (1940)
51. H.M.F. Freundlich, Z. Phys, Chem. **57**, 385 (1906)
52. M. Ghaedj, F. Karimi, B. Barrazzch, R. Sahraei, A. Danichfar, J. Ind. Eng. Chem. **19**, 756 (2013)
53. A. Ahmad, M. Rafatullah, O. Sulaiman, M.H. Ibrahim, R. Hashim, J. Hazard. Mater **170**, 357 (2009)
54. M. Ghaedi, A. Ansari, M.H. Habibi, A.R. Asghari, J. Ind. Eng. Chem. **20**(1), 17 (2014)
55. D. Robati, M. Rajabi, O. Moradi, F. Najafi, I. Tyagi, S. Agarwal, V.K. Gupta, J. Mol. Liq **214**, 259 (2016)
56. T.A. Khan, M. Nazir, Environ. Prog. Sustain Energy **34**, 1444 (2015)
57. M. Ghaedi, E. Nazari, R. Sahrai, M.K. Purkait, Desalin. Water Treat. **52**, 5504 (2014)
58. S.I. Abubaker, M.B. Ibrahim, J. Pure Appl. Sci. **11**, 273 (2018)
59. A.E. Adnan, T.A. Selman, Res. J. Pharm. Biol. Chem. Sci. **7**, 591 (2016)
60. S.H. Lubbad, B.K.A. Al-Roos, F.S. Kodeh, Curr. Green Chem. **6**, 53 (2019)